The observation of speckle using X-rays opens up many exciting possibilities for future work. In particular, by measuring the evolution of the speckle pattern in time, we can carry out X-ray intensity fluctuation spectroscopy. This technique not only measures the dynamics of nonequilibrium systems but is also one of the few techniques that can directly measure the dynamics of equilibrium systems. One important class of applications is the study of mass-transport mechanisms on length scales of 1–100 nm in materials such as metal alloys and complex fluids[8]. Of immediate interest are critical phenomena in equilibrium dynamics[9] and fluctuations during nonequilibrium domain coarsening[10]. Another class is the study of phason dynamics in materials with an incommensurate modulation, such as charge-density-wave systems and quasicrystals.

The present measurements using X25 at NSLS give a maximum count rate of 10 counts per s, allowing the study of correlation times down to 0.1 s. Such timescales are relevant to mass transport over all distances down to the atomic scale in typical solids at temperatures below about half their melting point. New undulator-based facilities at the European synchrotron radiation facility, the advanced photon source and elsewhere will provide an increase of three orders of magnitude in coherent intensity. This will enable studies probing correlation times in the microsecond range and studies of materials that scatter relatively weakly.

Intensity fluctuation spectroscopy does not make full use of the structural information in the speckle pattern. In principle, the speckle pattern contains complete information on the disordered structure producing it[6]. This structure could be imaged by Fourier inversion. In some cases, such as single grain boundaries or dislocations, the speckle pattern will be relatively simple, and one could use it to determine the atomic structure of these defects. □

Received 25 February; accepted 25 June 1991.

1. Pusey, P. N. in *Photon Correlation Spectroscopy and Velocimetry* (eds Cummins, H. Z. & Pike, E. R.) 45–141 (Plenum, New York, 1977).
2. Jakeman, E., Pusey, P. N. & Vaughan, J. M. *Opt. Commun.* **17,** 305–308 (1976).
3. Born, M. & Wolf, E. *Principles of Optics* 396; 511 (Pergamon, Oxford, 1975).
4. Rarback, H., Jacobsen, C., Kirz, J. & McNulty, I. *Nucl. Instrum. Meth.* A**266,** 96–105 (1988).
5. Berman, L. E. & Hart, M. *Nucl. Instrum. Meth.* A**300,** 415–421 (1991).
6. Ludwig, K. F. Jr. *Phys. Rev. Lett.* **61,** 1526 (1988).
7. Warren, B. E. *X-ray Diffraction,* 206–247 (Dover, Minoela, New York, 1990).
8. Lipowsky, R. *Nature* **349,** 475–481 (1990).
9. Hohenberg, P. C. & Halperin, B. I. *Rev. mod. Phys.* **49,** 435–479 (1977).
10. Roland, C. & Grant, M. *Phys. Rev. Lett.* **63,** 551–554 (1989).

ACKNOWLEDGEMENTS. We thank M. Grant for discussions and R. Sweet, Jia Wang, B. Ocko and R. Shannon for their help.

# Transition from a uniform state to hexagonal and striped Turing patterns

**Q. Ouyang & Harry L. Swinney**

Center for Nonlinear Dynamics and Department of Physics, The University of Texas, Austin, Texas 78712, USA

**CHEMICAL travelling waves have been studied experimentally for more than two decades[1–5], but the stationary patterns predicted by Turing[6] in 1952 were observed only recently[7–9], as patterns localized along a band in a gel reactor containing a concentration gradient in reagents. The observations are consistent with a mathematical model for their geometry of reactor[10] (see also ref. 11). Here we report the observation of extended (quasi-two-dimensional) Turing patterns and of a Turing bifurcation—a transition, as a control parameter is varied, from a spatially uniform state to a patterned state. These patterns form spontaneously in a thin disc-shaped gel in contact with a reservoir of reagents of the chlorite–iodide–malonic acid reaction[12]. Figure 1 shows examples of the hexagonal, striped and mixed patterns that can occur. Turing patterns have similarities to hydrodynamic patterns (see, for example, ref. 13), but are of particular interest because they possess an intrinsic wavelength and have a possible relationship to biological patterns[14–17].**

The reaction medium is a 2.0-mm-thick polyacrylamide gel disk (25.4-mm diameter), which is sandwiched between two 0.4-mm-thick porous glass disks (Vycor glass, Corning); similar reactors have been described previously[5,18]. The gel was prepared by the procedure in ref. 7. The gel and glass disks are transparent; the pattern can therefore be detected optically. The outer flat surface of each glass disk is in contact with a chemical reservoir, where reactant concentrations are kept constant and uniform by mixing and a continuous flow of fresh reagents. Components of the chlorite–iodide–malonic acid reaction[12] are distributed in the two reservoirs in such a way that neither is separately reactive. The chemicals diffuse through the porous glass disks into the gel where the reaction occurs. The gel, loaded with a soluble starch indicator (Thiodène, Prolabo), changes colour from yellow to blue with changes in concentration of $I_3^-$ during the redox reaction. No starch is present in the porous glass; thus concentration changes in the glass disks are not visible. The pattern is monitored in transmitted light (580 nm) with a video camera.

Beyond critical values of the control parameters (chemical concentrations and temperature), patterns emerge spontaneously from an initially uniform background. Initially, after the parameters are switched into a regime where patterns arise,

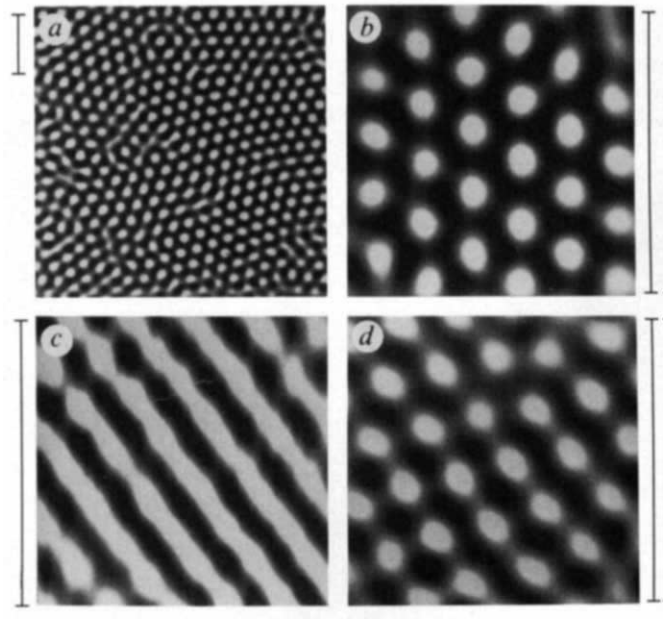


FIG. 1 Stationary chemical patterns formed in a continuously fed laboratory reactor. *a, b,* Hexagons; *c,* stripes; *d,* mixed state. The bar beside each picture represents 1 mm; the reactor is 25 mm in diameter. The concentrations in reservoirs A and B on the two sides of the reactor were: $[I^-]_0^A$, $[I^-]_0^B$, $[CH_2(COOH)_2]_0^B$ (in $10^{-3}$M) in *a* and *d,* 3.0, 3.0, 13; in *b,* 3.5, 3.5, 8.3; in *c,* 5.0, 5.0, 8.3 (for the conditions given, the mixed state in *d* coexists with the hexagons in *a*). The parameters common to all observed patterns were: $[NaOH]_0^A = [NaOH]_0^B = 3.0 \times 10^{-3}$ M, $[Na_2SO_4]_0^A = [Na_2SO_4]_0^B = 3.0 \times 10^{-3}$ M, $[ClO_2^-]_0^A = 1.8 \times 10^{-2}$ M, $[ClO_2^-]_0^B = 0$, $[CH_2(COOH)_2]_0^A = 0$, $[H_2SO_4]_0^A = 2.0 \times 10^{-3}$ M, $[H_2SO_4]_0^B = 1.0 \times 10^{-2}$ M, temperature 5.6 °C.

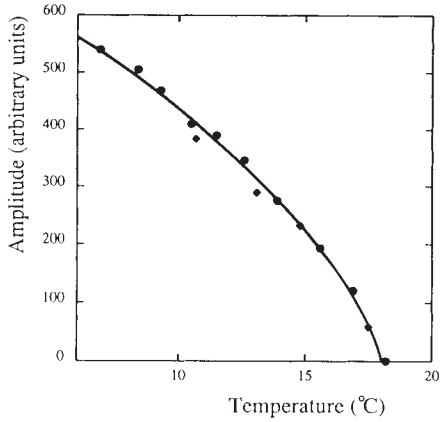


FIG. 2 The transition from a uniform state to a hexagonal Turing pattern. The amplitude was obtained from the modulus of a two-dimensional Fourier transform of a band near the spatial frequency 5.6 $mm^{-1}$. The points ● (◆) were measured for temperature decreasing (increasing) in steps. Concentrations were the same as in Fig. 1*b* except that $[ClO_2^-]_0^A = 2.0 \times 10^{-2}$ M.

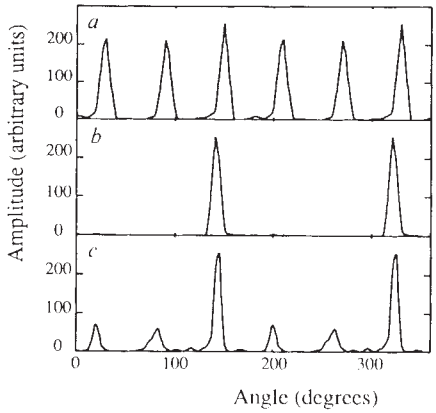


FIG. 3 Angular intensity distributions in spatial frequency space (in a band centred at 5.6 $mm^{-1}$) for *a*, hexagons, *b*, stripes and *c*, mixed state. Conditions for *a*, *b* and *c* respectively correspond to the conditions in Fig. 1*b*, *c* and *d*.

there are many (~100) transient yellow circles growing in a blue background. Within an hour these patterns slowly stop propagating and break up into yellow dot patterns which evolve more slowly. The system approaches a nearly stationary state with domains of hexagonal patterns (Fig. 1*b*) separated by grain boundaries (Fig. 1*a*) which move very slowly, typically only 0.2 mm per day.

The transition from the uniform state to a hexagonal pattern was studied with temperature as a control parameter and other parameters held fixed: the hexagonal pattern emerged as the temperature was lowered, as Fig. 2 illustrates. Within the experimental resolution there was no hysteresis; the transition occurred at 18.0 ± 0.5 °C for both increasing and decreasing temperature. The system showed a critical slowing down at temperatures near the transition: the relaxation time became days, whereas far from the transition (for example at 5.6 °C) the system relaxed within 3 hours. These observations suggest that the transition is continuous, but a small discontinuity, as expected from theory (to be discussed), would not be observable with our resolution.

Stripes rather than hexagons were observed at high iodide or low malonic acid concentration. The stripes (Fig. 1*c*) were stationary, in contrast to the widely studied travelling wave patterns[1–5]. Striped patterns were maintained for days without much change except for a very slow motion of the grain boundaries separating different domains.

The wavelengths of the hexagonal and striped patterns, determined from spatial fast Fourier transforms, varied continuously from 0.14 to 0.33 mm with changes in the control parameters. The wavelength is an intrinsic property of the reaction-diffusion system, not a consequence of finite size of the system. This intrinsic wavelength distinguishes Turing patterns from other well known nonequilibrium structures such as convection rolls or Taylor vortices. The wavelength was especially sensitive to the sulphuric acid concentration in reservoir A; for example a decrease of sulphuric acid concentration in reservoir A by 33% led to a 45% increase in wavelength of the hexagons and stripes.

A distinct stable mixed state was observed as well as the pure hexagons and stripes. Mixed states are discernible in photographs, as in Fig. 1*d*, and can be quantified in graphs of the angular distribution of amplitude (Fig. 3). Pure hexagons have six peaks of equal amplitude separated by 60° (Fig. 3*a*); pure stripes have two peaks separated by 180° (Fig. 3*b*); and the observed mixed state has six peaks separated by 60°, with one large peak followed by two small, one large, and two small (Fig. 3*c*).

Two-dimensional chemical patterns similar to those we have observed have been found in numerical simulations of reaction-diffusion models with the kinetics given by the Brusselator[19] or variants[20] or by an activator-inhibitor[21] model. Pattern formation in two-dimensional systems has also been extensively studied using general equations that describe the amplitude of the patterns[22]. In the absence of specific symmetries, which is the usual situation in chemistry, the initial transition from a uniform state to hexagons is discontinuous[23–25]. But in practice the sizes of the discontinuity and hysteresis range are usually small, and the transition shares most features with a continuous transition. Simulations by V. Dufiet and J. Boissonade (personal communication) on a two-species reaction-diffusion model[26] reveal a transition with a hysteresis that is only 0.1% of the control parameter, too small to observe with our experimental resolution.

Our experiments show evidence of a transition to Turing patterns that can be maintained indefinitely in a well-defined nonequilibrium state. We have neglected possible structure in the direction of the chemical gradient; such structure might exist, as the thickness of the gel is 6–10 times as great as the wavelength of the pattern. Walgraef *et al.*[27] have shown that in three-dimensional systems with no imposed gradients, the most likely selected patterns should be body-centred cubic, hexagonal prisms and stripes, all of which have been found in simulations (A. DeWit *et al.*, personal communication). Only the body-centred cubic pattern has structure in three dimensions; the patterns we have observed, hexagons and stripes, have no three-dimensional structure.

Further experiments are under way to search for the other types of patterns and to study the transitions between patterns, multi-stability, the dynamics of defects and the role of three-dimensionality. The development of continuously fed spatially extended reactors such as the one described here opens a wide range of problems to systematic laboratory study. □

Received 22 April; accepted 14 June 1991.

1. Zaikin, A. N. & Zhabotinskii, A. M. *Nature* **225,** 535–537 (1970).
2. Field, R. J. & Berger, M. (eds) *Oscillations and Traveling Waves in Chemical Systems* (Wiley, New York, 1985).
3. Winfree, A. T. *When Time Breaks Down* (Princeton University Press, 1987).
4. Tyson, J. J. & Keener, J. P. *Physica* D**32,** 327–361 (1988).
5. Noszticzius, Z., Horsthemke, W., McCormick, W. D., Swinney, H. L. & Tam, W. Y. *Nature* **329,** 619–620 (1987).
6. Turing, A. M. *Phil. Trans. R. Soc. Lond.* B**327,** 37–72 (1952).
7. Castets, V., Dulos, E., Boissonade, J. & de Kepper, P. *Phys. Rev. Lett.* **64,** 2953–2956 (1990).
8. Boissonade, J., Castets, V., Dulos, E. & de Kepper, P. *ISNM* **97,** 67–77 (Birkhäuser, Basel, 1991).
9. De Kepper, P., Castets, V., Dulos, E. & Boissonade, J. *Physica* D**49,** 161–169 (1991).
10. Boissonade, J. *J. Phys.* **49,** 541–546 (1988).
11. Lengyel, I. & Epstein, I. R. *Science* **251,** 650–652 (1991).
12. De Kepper, P., Boissonade, J. & Epstein, I. R. *J. phys. Chem.* **94,** 6525–6536 (1990).
13. White, D. B. *J. Fluid Mech.* **191,** 247–286 (1988).

14. Nicolis, G. & Prigogine, I. *Self-Organization in Nonequilibrium Systems* (Wiley, New York, 1977).
15. Meinhardt, H. *Models of Biological Pattern Formation* (Academic New York, 1982).
16. Harrison, L. G. *J. theor. Biol.* **125,** 369–384 (1987).
17. Murray, J. D. *Mathematical Biology* (Springer, Berlin, 1989).
18. Kshirsagar, G., Noszticzius, Z., McCormick, W. & Swinney, H. L. *Physica* D**49,** 5–12 (1991).
19. Borckmans, P., Dewel, G. & De Wit, A in *Seeds: Genesis of Natural and Artificial Forms,* 62–71 (Le Biopole Végétal, Amiens, 1991).
20. Lacalli, T. C., Wilkinson, D. A. & Harrison, L. C. *Development* **104,** 105–113 (1988).
21. Haken, H. & Olbrich, H. *J. math. Biol.* **6,** 317–331 (1978).
22. Mannerville, P. *Dissipative Structures and Weak Turbulence* (Academic, Boston, 1990).
23. Busse, F. H. *J. Fluid Mech.* **30,** 625–649 (1967).
24. Pismen, L. M. *J. chem. Phys.* **72,** 1900–1907 (1980).
25. Malomed, B. A. & Tribel'skii, M. I. *Sov. Phys. JETP* **65,** 3013–3016 (1987).
26. Schnackenberg, J. *J. theor. Biol.* **81,** 389–400 (1979).
27. Walgraef, D., Dewel, G. & Borckmans, P. *Phys. Rev.* A**21,** 397–404 (1980); *Adv. chem. Phys.* **49,** 311–355 (1982).

ACKNOWLEDGEMENTS. We thank J. Boissonade and V. Dufiet for numerical simulations and for comments on the manuscript, and A. Armeodo, P. Borchmans, P. de Kepper, G. Dewel, A. de Wit, W. McCormick, D. Vigil and D. Walgraef for discussions. This work was supported by the US Department of Energy Office of Basic Energy Sciences and BP Venture Research.

# High turnover rates of dissolved organic carbon during a spring phytoplankton bloom

**David L. Kirchman*, Yoshimi Suzuki†, Christopher Garside‡ & Hugh W. Ducklow§**

* College of Marine Studies, University of Delaware, Lewes, Delaware 19958, USA
† Geochemical Laboratory, Meteorological Research Institute, Nagamine 1-1 Tsukuba-shi, Ibaraki, 305 Japan
‡ Bigelow Laboratory, West Boothbay Harbor, Maine 04575, USA
§ Horn Point Environmental Laboratory, University of Maryland, Cambridge, Maryland 21613, USA

**OCEANIC dissolved organic carbon (DOC) is one of the Earth's largest carbon reservoirs, but until recently its role in the carbon cycle has been neglected. New methodology[1], however, has led to larger estimates of DOC concentrations and also to renewed interest in the biochemical lability of DOC[2]. Previous work found that the mean age of DOC in the surface ocean was >1,000 years[3]. To examine the lability of DOC in greater detail, we have conducted experiments to estimate DOC turnover rates in the upper ocean. We directly observed rapid DOC turnover by bacterioplankton during the spring phytoplankton bloom in the North Atlantic ocean. Potential turnover rates, measured in 0.8-μm filtered samples, ranged from 0.025 to 0.363 per day, and were consistent with bacterial biomass production and uptake of dissolved nitrogen ($NH_4^+$, $NO_3^-$ and urea). Our results indirectly suggest that cycling of dissolved organic nitrogen (DON) differs from that of DOC. The high estimates of DOC concentrations and turnover rates repeated here, if found to be general, would seem to demand changes in models[4] of carbon cycling and of the ocean's role in buffering increases in atmospheric $CO_2$.**

Our experiments were conducted as part of the Joint Global Ocean Flux Study (JGOFS), which had the objective of examining the 1989 spring phytoplankton bloom in the North Atlantic Ocean (47° N; 18° W) and its role in the ocean carbon cycle[5]. The bloom started in late April, as indicated by increases in chlorophyll *a* and decreases in $NO_3^-$ and total inorganic carbon. It continued until at least early June, sustained by ammonium recycling and residual $NO_3^-$. To examine the possible rate of degradation of DOC, we gravity-filtered surface sea water through Nuclepore filters with pore sizes of 0.8 μm (diameter 142 mm), added an equal volume of the same water filtered through 0.22-μm Millipore filters (which remove all microorganisms) and then incubated this mixture in the dark at ambient temperature (~14 °C). All filters were rinsed with distilled water and sample water before use. The 0.8-μm filtrate contained nearly the entire heterotrophic bacterial assemblage and only 10% of chlorophyll *a*; that is, initially it did not contain sources of DOC (phytoplankton and zooplankton) although it retained those organisms (bacteria) thought to be mainly responsible for DOC oxidation.

Bacterial abundance (measured by direct counts[6]) increased with time (Fig. 1*a*), because 0.8-μm filtration excludes many grazers of bacteria, and dilution further minimizes bacterivore activity[7,8]. After 4.2 days, the bacterial abundance decreased because bacterivorous microflagellates increased from initially very low numbers to populations that had a considerable effect on the bacteria (Fig. 1*a*). Accompanying the initial increase in bacterial abundance, there was a decrease in DOC concentrations (measured by high-temperature catalytic oxidation[1]) in these <0.8-μm filtrates (Fig. 1*b*). For the first day, the apparent rate of DOC degradation was high, ~0.2 per day (Table 1; rates are first-order decay constants). The rate decreased during the incubation period (Fig. 1b), and rates were lower when calculated over intervals greater than 2 days (Table 1). The lowest turnover rate of DOC was 0.025 ± 0.005 per day, estimated after 4.2 days in an incubation lasting 11 days. At least some of the apparent decrease in turnover rates was probably related to the increase in bacterivore activity. Grazing by bacterivores lowers bacterial abundance and releases DOC[9], thus slowing its net depletion. Even so, our lowest turnover rate is still greater than those estimated in previous studies[10,11] similar to ours.

The high DOC turnover rates did not result from the release of labile DOC during filtration. Concentrations of DOC before and after filtration were similar, indicating that any DOC contamination was small. Also, the fraction of DOC consumed in these experiments (23–42%; Table 1) is too high to be explained by degradation of the small amount (nM) of DOC perhaps released by cell lysis during filtration. Although our estimates at the end of these experiments did approach the low DOC concentrations measured by the wet-combustion method (*in situ* concentrations measured by this method[12] are about half those measured by high-temperature catalytic oxidation), our incubations probably did not last long enough to determine what fraction of the DOC was highly refractory with low turnover rates. Nonetheless, the lowest initial DOC turnover rate did coincide with the lowest initial concentration (31 May; Table 1). In short, our results indicate that DOC is more labile in surface waters than indicated by previous estimates of DOC age and turnover[3,10,11].

Bacterial activity (and possibly that of other microorganisms) was essential to deplete the DOC concentrations in the 0.8-μm filtrates. The concentrations of DOC did not decrease when sea water was filtered through 0.22-μm Millipore filters, which remove all microorganisms (Fig. 1*b*), indicating that the decrease was not due to adsorption on the container walls or abiotic oxidation.

The nitrogen required for the observed bacterial growth was apparently supplied by $NH_4^+$, $NO_3^-$ and urea. The concentrations of these nitrogenous compounds decreased during periods when

TABLE 1 Summary of dissolved organic carbon (DOC) turnover rates calculated from DOC depletion in <0.8-μm filtrates

| Start date (1989) | Incubation period (d) | Initial DOC (μM) | Fraction consumed (%) | Turnover rate ($d^{-1}$)* | *n* |
|---|---|---|---|---|---|
| 25 May | 0–1.0 | 196 ± 8 | | 0.230 ± 0.020 | 4 |
| | 1.0–4.2 | 155 ± 3 | | 0.048 ± 0.003 | 6 |
| | 4.2–11 | 134 ± 1 | 42 | 0.025 ± 0.005 | 4 |
| 28 May | 0–1.0 | 178 ± 2 | | 0.363 ± 0.290 | 3 |
| | 1.3–4.0 | 146 ± 2 | 28 | 0.044 ± 0.009 | 4 |
| 31 May | 0–3.0 | 136 ± 3 | 23 | 0.087 ± 0.017 | 5 |

* Turnover rates were calculated by applying first-order kinetics to incubation periods during which graphs of ln (DOC concentration) against time were linear. The rate is then the slope of that line (±standard error) calculated with *n* time points.